Special section: Geophysical monitorings at the Earth's polar regions

Advances in seismic monitoring at Deception Island volcano (Antarctica) since the International Polar Year

Enrique Carmona[1], Javier Almendros[1,2,*], Rosa Martín[1], Guillermo Cortés[1], Gerardo Alguacil[1,2], Javier Moreno[1], José Benito Martín[1], Antonio Martos[1], Inmaculada Serrano[1,2], Daniel Stich[1,2], Jesús M. Ibáñez[1,2]

[1] Instituto Andaluz de Geofísica, Universidad de Granada, Granada, Spain

[2] Departamento de Física Teórica y del Cosmos, Universidad de Granada, Granada, Spain

ABSTRACT

Deception Island is an active volcano located in the south Shetland Islands, Antarctica. It constitutes a natural laboratory to test geophysical instruments in extreme conditions, since they have to endure not only the Antarctic climate but also the volcanic environment. Deception is one of the most visited places in Antarctica, both by scientists and tourists, which emphasize the importance of volcano monitoring. Seismic monitoring has been going on since 1986 during austral summer surveys. The recorded data include volcano-tectonic earthquakes, long-period events and volcanic tremor, among others. The level of seismicity ranges from quiet periods to seismic crises (e.g. 1992-1993, 1999). Our group has been involved in volcano monitoring at Deception Island since 1994. Based on this experience, in recent years we have made the most of the opportunities of the International Polar Year 2007-2008 to introduce advances in seismic monitoring along four lines: (1) the improvement of the seismic network installed for seismic monitoring during the summer surveys; (2) the development and improvement of seismic arrays for the detection and characterization of seismo-volcanic signals; (3) the design of automated event recognition tools, to simplify the process of data interpretation; and (4) the deployment of permanent seismic stations. These advances help us to obtain more data of better quality, and therefore to improve our interpretation of the seismo-volcanic activity at Deception Island, which is a crucial step in terms of hazards assessment.

1. Introduction

Deception Island is located in the Bransfield Strait between the South Shetland Islands and the Antarctic Peninsula (Figure 1). It is an active volcano with recent eruptions, continuous fumarolic activity, thermal anomalies, and a moderate level of volcano seismicity. There are two functioning scientific bases (Argentinian and Spanish) in the island, generally operating during Antarctic summers. Deception is one of the most visited places in Antarctica both by scientists and tourists, which emphasizes the importance of volcano surveillance and monitoring.
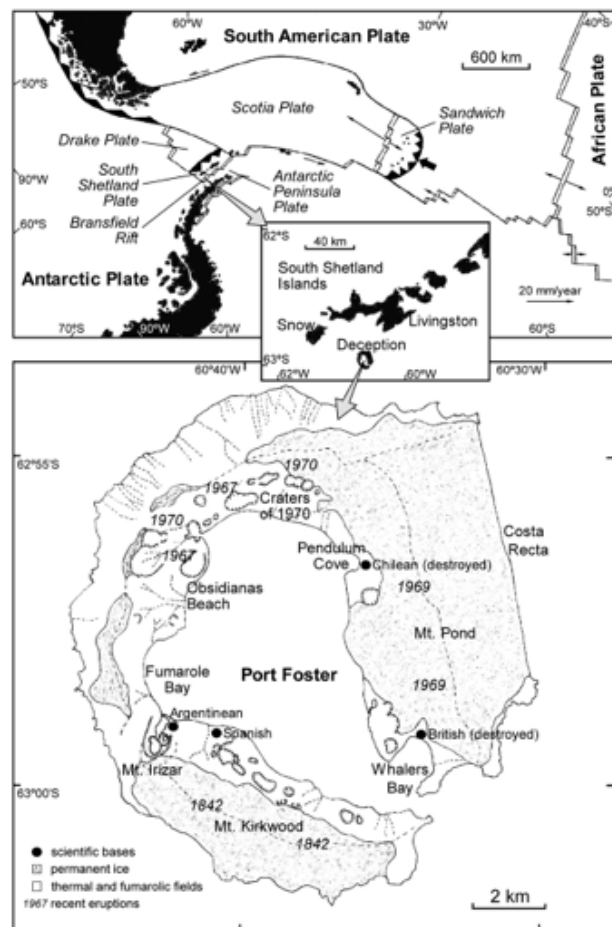

Figure 1. Simplified tectonic map showing the location of Deception Island in the South Shetland Island region and map of Deception Island with indication of the main volcanic features.

In particular, seismic monitoring at Deception Island has been going on during austral summer surveys since 1986, mostly performed by Argentinian and Spanish teams. Our research group of the Instituto Andaluz de Geofísica, University of Granada, Spain (IAG-UGR) is involved in volcano monitoring at Deception Island since 1994, in collaboration with other Spanish and international groups. The Antarctic climate and volcanic environment make of Deception Island a natural laboratory adequate to test geophysical instruments in extreme conditions. Based on this experience, in recent years we have introduced several advances in seismic monitoring, prompted by the opportunities offered by the International Polar Year (IPY) 2007-2008. The IPY was an international scientific initiative intended to promote and support polar research. Spain, as most participating countries, provided a special line of funding for IPY-related projects, which allowed us to update and improve our instruments and monitoring techniques.

In this paper, we describe advances in seismic monitoring at Deception Island volcano carried out since the IPY 2007-2008. First of all, we updated the seismic network installed during the summer surveys for volcano monitoring. We now use three-component stations, 24-bit data acquisition systems, and real-time data telemetry to a recording centre via wireless connections. These systems are more efficient in terms of power, and require less maintenance, than the instruments we used before. We have also developed efficient 12-channel seismic arrays, intended for the detection and characterization of seismo-volcanic signals. To simplify and speed up data interpretation, we have designed and trained automated event recognition tools. Finally, we extended the temporal coverage with the deployment of a permanent seismic station at Deception Island, along with other two stations at Livingston Island and Cierva Cove. These advances help us to obtain more data of better quality, and therefore to improve our interpretation of the seismo-volcanic activity, which is crucial for hazards assessment.

2. Geological and geophysical setting

Deception Island volcano (Figure 1) lies in an area of complex tectonic interactions between the south-American and Antarctic plates and the Scotia, Drake, and South Shetlands microplates [Pelayo and Wiens 1989, Baraldo and Rinaldi 2000, Robertson-Maurice et al. 2003]. Deception is situated near the spreading axis of the Bransfield Rift. It is considered one of the most active volcanoes in Antarctica with recent eruptions occurred in 1967-1970 [Smellie 1988]. The island has a horseshoe shape with diameter of 15 km and a flooded inner bay. Several theories have been proposed to explain the origin of the Deception Island caldera. We can mention a catastrophic collapse after one or more major eruptions of andesitic magma [Baker et al. 1975, Smellie 1988]; the incremental growth in response to a series of moderate-sized eruptions [Walker 1984]; and a tectonic depression caused by extensional movements along normal faults following the regional trends [Rey et al. 1995, Martí et al. 1996, González-Casado et al. 1999].

Field mapping and seismic reflection studies have shown the presence of three major fault systems in Deception Island [Rey et al. 1995, Martí et al. 1996]: a NE-SW system, parallel to the axis of the Bransfield Rift; a roughly E-W system including several alignments formed during historical eruptions; and a NNW-SSE system, coincident with other alignments such as Costa Recta [Fernández-Ibáñez et al. 2005], the impressive linear feature that shapes the eastern coastline of Deception Island (Figure 1).

Historical eruptions at Deception Island (Figure 1) have been relatively small in terms of volume of emitted material. The first one took place in 1842 [Roobol 1973], while the last series of eruptions occurred in December 1967, with two major eruptive centres in the northwestern sector; in February 1969, with the opening of a fissure in the eastern side of the island; and in August 1970, when several aligned cones formed in the northern sector [Smellie and López-Martínez 2002].

Associated with volcanic activity, we find geothermal areas and gas emissions near the inner shore of the island [Caselli et al. 2007]. Studies of thermal anomalies and gas emissions show increases in SO_2 flux after periods with enhanced seismic activity, for example after the 1999 seismic crisis and during the 2003-2004 survey. Caselli et al. [2004, 2007] interpreted these phenomena as a consequence of dike intrusions into the surface layers. After the seismic crisis of 1999, there was also a change from extension and uplift of the entire island to compression and subsidence in the northern and northwestern areas [Berrocoso et al. 2008].

Seismic studies have demonstrated that the internal structure of Deception Island is highly heterogeneous. Saccorotti et al. [2001] found strong lateral contrast of seismic velocity between the old caldera structure and the recent volcanic deposits. Martínez-Arévalo et al. [2003] showed that the first few kilometres of the crust beneath the inner bay are highly fractured and anisotropic, which strongly affects seismic wave propagation [e.g. Havskov et al. 2003]. Zandomeneghi et al. [2009] suggested the presence of a shallow magma chamber under Port Foster bay, based on results of high-resolution P-wave seismic tomography. García-Yeguas et al. [2011]
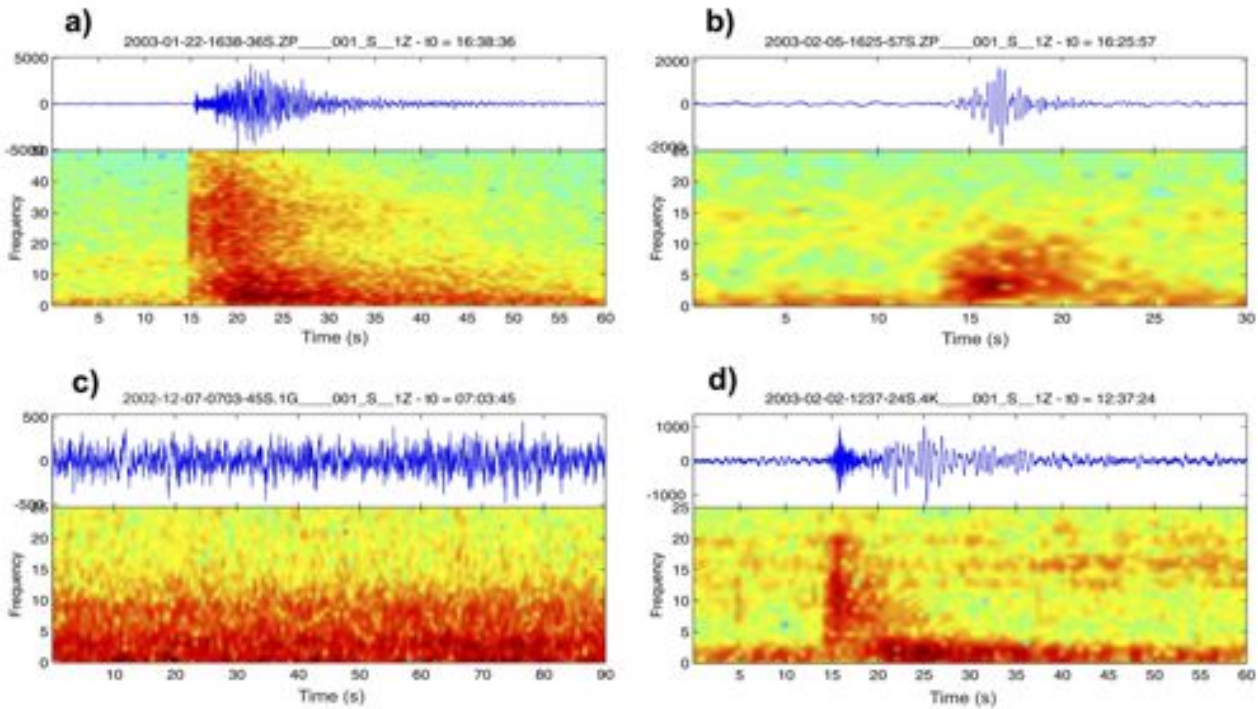
Figure 2. Examples of vertical-component seismograms and spectrograms recorded at Deception Island: (a) VT earthquake; (b) LP event with frequency content centered at 2.5 Hz; (c) volcanic tremor; (d) hybrid event.

used array analyses to study anomalies in seismic wave propagation for different areas inside the bay, which can only be explained by the effect of heterogeneous structure. Luzón et al. [2011] found marked differences in the shallow velocity structure in different parts of the island, due to the occurrence of hydrothermal activity and to the presence of compact pre-caldera materials.

Deception Island has a moderate background of seismic activity. As in most volcanoes, seismic signals are quite diverse. They can be divided in two main groups: volcano-tectonic (VT) earthquakes and long-period (LP) seismicity. Hybrid events have been also occasionally recorded.

VT earthquakes are shallow earthquakes with S-P time differences less than 4 s and a broad spectral content reaching frequencies up to 30 Hz (Figure 2a). They are caused by brittle rock failures under stresses related to the internal dynamics of the volcano. These earthquakes are spatially distributed throughout the island, although some seismic swarms concentrate in specific areas [Ibáñez et al. 2003b, Carmona et al. 2012]. The study of VT earthquakes provides information on the local stress state and source dynamics [Ibáñez et al. 2003a,b, Almendros et al. 2004, Carmona et al. 2010].

LP seismicity includes LP events and volcanic tremor [Chouet 1996]. They originate from interactions between the solid rock and the fluid dynamics within the volcano. LP events usually have durations ranging from a few seconds to a minute. The spectral content is quasi-monochromatic, with one or more peaks below 5 Hz (Figure 2b). They have a spindle-shaped envelope and

emergent phase arrivals. Volcanic tremor (Figure 2c) has similar characteristics to LP events, although it has a longer duration that may reach up to hours and days. LP events and tremor are the most characteristic seismic signals recorded in volcanic areas. Their origin is attributed to resonance of fluid-filled conduits, oscillations of fluid flow, etc. [Chouet 1992, Julian 1994, Konstantinou and Schlindwein 2002].

Hybrid events (Figure 2d) are a transition class between LP events and VT earthquakes and share characteristics of both event types [Lahr et al. 1994]. They are apparently composed by a VT earthquake followed by an LP event. Their origin is similar to the LP events, although in this case the resonance of fluid-filled conduits is triggered by a VT earthquake [Ibáñez et al. 2003b].

The level of seismicity is highly variable and ranges from quiet periods to seismic crises. For example, seismic activity from 1986 to 1991 was scarce and of low energy. However, in January-February 1992 it increased significantly with 776 recorded VTs, and was accompanied by gravity variations [Ortiz et al. 1992, 1997, García et al. 1997]. The next year, seismic activity fell back to normal levels [Ibáñez et al. 2003a]. Another substantial increase in seismic activity occurred at the beginning of 1999. Seismic stations recorded a total of 3643 events: 2072 VT earthquakes with magnitudes between −0.8 and 3.4 [Ibáñez et al. 2003b], 1556 LP events, and a few hybrids and tremor episodes [Ibáñez et al. 2003a,b]. Two of the VT earthquakes were felt by the staff of the Gabriel de Castilla Spanish Base. Analyses of this seismic activity demonstrate that LP seismicity was unre-

lated to VT earthquakes [Ibáñez et al. 2003a]. While LPs were of hydrothermal origin, VTs were probably produced by the reactivation of a magma chamber which destabilized the local stress field. Some groups of VT earthquakes were suitable for precise relocation, and the associated rupture planes have been identified [Almendros et al. 2004, Carmona et al. 2010].

In the surveys following the 1999 seismo-volcanic crisis, seismic activity was characterized by a predominance of LP events [Carmona et al. 2012]. The number of LP events was highly variable: we recorded 2868 LP events during the 2003-2004 survey, the largest number since we started monitoring in 1994, and only 58 LPs during the 2007-2008 survey. VT activity was at normal levels, quite below the two crises occurred in 1992 and 1999. Several tens of VTs generally occur during every survey, except for the 2004-2005 and 2008-2009 surveys when we recorded a smaller number of VT earthquakes. Volcanic tremor was always present except during the two surveys with lowest activity (2004-2005 and 2008-2009) and 2010-2011.

These observations suggest that Deception Island volcano is at present in a state characterized by low-energy LP events and episodes of volcanic tremor caused by circulation of fluids in the hydrothermal system. A few VT and hybrid events may also occur as a local response to the regional tectonics [Carmona et al. 2012]. However, recent eruptions and the evidence of sustained volcanic activity provided by geophysical, geochemical and geodetic observations (i.e. changes in groundwater systems, gas emissions, thermal anomalies, surface deformations, and seismic activity) reveal that Deception Island poses a significant hazard. The presence of two scientific bases and an ever-increasing tourism emphasize the need of a permanent volcano monitoring.

3. Seismic monitoring before the International Polar Year (1994-2007)

Seismic monitoring at Deception Island started in the mid 1950's with the installation of a seismometer at the Argentinean Base, but it was interrupted after the late 1960's eruptions. In 1986, an Argentinean-Spanish research group restarted seismic monitoring with the installation of short-period stations [Vila et al. 1992, 1995, Correig et al. 1997, Ortiz et al. 1997].

Our group joined the seismic investigations at Deception Island in 1994, with the installation of seismic arrays for research and monitoring. From that time, we have been continuously involved in the seismic surveillance of the volcano [Almendros et al. 1997, 1999, Alguacil et al. 1999, Ibáñez et al. 1997, 2000, 2003b, Carmona et al. 2012]. Seismic surveys are periodically carried out during the three months of Antarctic summer, when the Gabriel de Castilla Base is open.

3.1. Instrumentation

The seismic instruments used at Deception Island have evolved since we started monitoring in 1994. Until 1999, our work was focused basically on the installation of small-aperture seismic arrays. They allow estimating the apparent slowness and propagation azimuth of the seismic wavefield, and are specially suited to study LP seismicity and low-magnitude VT earthquakes. We used 8-channel, 16-bit acquisition systems with GPS time, sampling at 200 sps [Havskov and Alguacil 2004]. Data recording was focused on seismic events and relied on a trigger detection algorithm (STA/LTA, short-term average over long-term average). Data were stored locally at the array site on a laptop computer. The seismometers were 4.5 Hz Mark Products L15 or L28, with a response electronically extended to 1 Hz. We also deployed a short-period station equipped with a vertical-component, 1 Hz Mark Products L4C seismometer near the Spanish Base, with real-time data visualization for the seismic surveillance of the volcano.

After the 1999 seismo-volcanic crisis, we combined the use of seismic arrays with the deployment of a short-period seismic network. We also deployed occasionally broadband seismometers, such as the Guralp CMG-40T, with a flat response from 30 s to 100 Hz. The short-period network was composed by 4 stations located in different points of interest around Port Foster. Three of them had a vertical-component Mark Products L4C seismometer with natural frequency of 1 Hz. From these stations data were transmitted through a radio telemetry system consisting of an analogue FM modulator and a VHF radio low-power transmitter with a directional antenna (Figure 3). At the Spanish Base, the received signals passed through a demodulator and a 16-bit A/D converter. Finally, data were digitally recorded in a raw format on a laptop computer [Ortiz et al. 1994]. The fourth station had a three-component, Mark Products L28 seismometer, with a response extended to 1 Hz. It was deployed near the Spanish Base, and connected by cable to the A/D converter. The radio transmission represented a breakthrough for the seismic monitoring of the volcano. However, its operation was sometimes affected by weather conditions. And since there was no local recording at the seismic station, any failure in the radio link implied loss of data.

Between 2003 and 2005, we developed a new acquisition system for the seismic arrays. It was based on a 24-bit A/D converter with GPS time, sampling 12 channels at 100 sps, with local recording on an industrial PC [Abril 2007]. Seismometers were Mark Products L28 with re-

Figure 3. Maintenance operations of a seismic network station during the 2003-2004 survey. Left: inspection of the radio telemetry antenna; right: battery replacement.

sponse electronically extended to 1 Hz. The most important feature of this system, apart from the increase of dynamic range and number of channels, is that it enables a continuous recording, which improves the array capabilities in case of low-energy signals and volcanic tremor.

The instrumentation deployed at Deception Island requires periodic maintenance because it wears out both during use and transportation. Except for commercial instruments, components and devices are designed and built by the IAG-UGR group. The equipments are usually shipped to Antarctica in September and return to Spain in May. In the four months preceding the next survey, we have to check, clean, and fine-tune the instruments. Apart from the normal decline due to use, the technological advances require continuous update of seismometers and acquisition systems. In this sense, we made the most of the International Polar Year opportunities to improve and upgrade our seismic instruments.

3.2. Data management
Until 2000, seismic data were recorded locally on field computers and downloaded manually during the periodic maintenance of the stations. Data were organized in different folders, sorted by date and station. The data visualization and phase picking were made using our own software, i.e. PICFASE [Guirao et al. 1990] and TAMBOR [Ortiz et al. 1994]. With the introduction of continuous recording we needed more powerful tools to manage the data. For this reason, we started using the SEISAN software package [Havskov and Ottemöller 1999] which includes a complete set of programs for seismic database management and earthquake analysis (phase picking, earthquake location, spectral analysis, estimate of source parameters), as well as graphical tools. All programs are tied to the same database. They run under Sun Solaris, Linux,

MacOS, and Microsoft Windows. SEISAN is able to read and convert to and from standard seismic data formats (SEISAN, GSE, SEED/miniSEED, SAC, ASCII). SEISAN is an open source code, available at the Seismology site of the University of Bergen, Norway (http://www.uib.no/rg/geodyn/artikler/2010/02/software).

Routine operations, such as format conversion and insertion of records into the database, are performed using scripts. Once data are in the proper database, the SEISAN tools are used to review and process them. Daily tasks carried out during the surveys at Deception Island are the identification and extraction of seismic events. This must be done as close to real-time as possible for surveillance purposes. Seismologists collaborate in the management of the volcanic colour alert code for Deception Island, providing information about current seismicity and possible changes in the volcanic activity pattern.

4. Seismic monitoring since the International Polar Year (2007-2011)
The most important advances achieved since the International Polar Year are related to the following aspects of seismic monitoring: data transmission, seismogram analysis, and temporal coverage. Improvements in data transmission allowed efficient real-time monitoring and the incorporation of seismic arrays into the surveillance network. Data analysis routines have been integrated in a single software package that performs automated analyses. Finally, the installation of a permanent station has allowed extending the temporal coverage of the recordings.

4.1. Seismic network
An important step to improve seismic monitoring at Deception Island was the modernization of the seismic network. Until 2007, the network was composed of

Figure 4. Left: SARA data acquisition system embedded in a waterproof PELI case; right: SARA data acquisition system and two batteries in an aluminum box for further protection.

vertical-component, short-period stations with radio telemetry and digital recording. During the International Polar Year, we designed and tested a new network of 4 stations based on digital dataloggers and WiFi data transmission. Stations were tested in the field during the 2008-2009 survey, and were fully operative in the 2009-2010 survey.

The new stations are based on 24-bit SL04 SARA dataloggers (Figure 4) sampling three channels at 100 sps. They use a PC with embedded Linux and the SeisLog acquisition software [Utheim and Havskov 1999]. SeisLog receives data from the A/D converter through a serial port. The data stream contains the three seismic channels and the GPS signal. Data are recorded in miniSEED format on an external pen drive. The acquisition software is based on a detection STA/LTA algorithm. SeisLog uses a LISS (Live Internet Seismic Server) to share data with other computers of the same network. We use two types of three-component seismometers: short-period Mark Products L4C with natural frequency of 1 Hz and medium-period Lennartz 3D/5s.

The design of the network is based on our experience at Deception Island, and takes into account both logistic and scientific aspects. Station sites must be easily accessible and far from obstacles that might interfere with the line-of-sight transmission to the Spanish Base. On the other hand, recent seismic activity has occurred mostly in the northern sector of Port Foster [Ibáñez et al. 2000, 2003b], where a magma chamber was imaged by Zandomeneghi et al. [2009]. Therefore, we deployed the seismic network to provide an optimum azimuthal coverage of the north half of Port Foster, at locations near the inner shore. Selected station sites are next to the Spanish Base (BASE), Obsidianas Beach (OBS), near the craters of the 1970 eruptions (C70), and the shelter of the Chilean Base, south of Pendulum Cove (CHI) (Figures 5 and 6).

Data acquisition systems are built inside a PELI

type case that protects them in bad weather conditions. Cases are placed, along with the batteries, in an aluminium alloy box (Figure 4). We take extra care in the choice of batteries of good quality and tolerant to low temperatures. To increase the autonomy of the stations, we use several batteries connected in parallel. Connections among batteries are fused and protected with a diode near the positive pole.

Seismometers are buried a few tens of centimetres below the ground. The actual depth that can be achieved is limited by the depth of the permafrost. Short-period sensors are versatile and can be deployed directly on the ground (Figure 7). Medium-period sensors are protected by aluminium pots filled with foam to reduce the external temperature variations (Figure 7). Proper levelling and orientation are achieved using a bubble level and compass, respectively.

Apart from the local storage of data, seismic stations are connected to a WiFi antenna that transmits data in real-time to the Spanish Base. We use Ubiquiti Networks Nanostation2 antennas. They are 2.4 GHz, dual-polarity, 10 dBi gain antennas, with a 54 Mbps transmission rate. Station antennas are mounted on a short pole near the acquisition system (Figure 8). They are oriented to face the Spanish Base, where a similar WiFi antenna is configured for reception. We have designed a circuit that allows independent power management for the seismic station and the wireless transmission. The objective is to prioritize data acquisition when battery is low. This circuit stops remote transmission when the battery level falls below a pre-defined threshold, in order to keep the seismic station running for a longer time.

The reception antenna located at the Gabriel de Castilla Base is connected to a computer running Seis-ComP 2.6 (Seismological Communication Processor by GFZ Postdam). This software supports several transmission protocols such as SeedLink, LISS, Guralp Scream, etc. It manages the visualization and recording of seismic
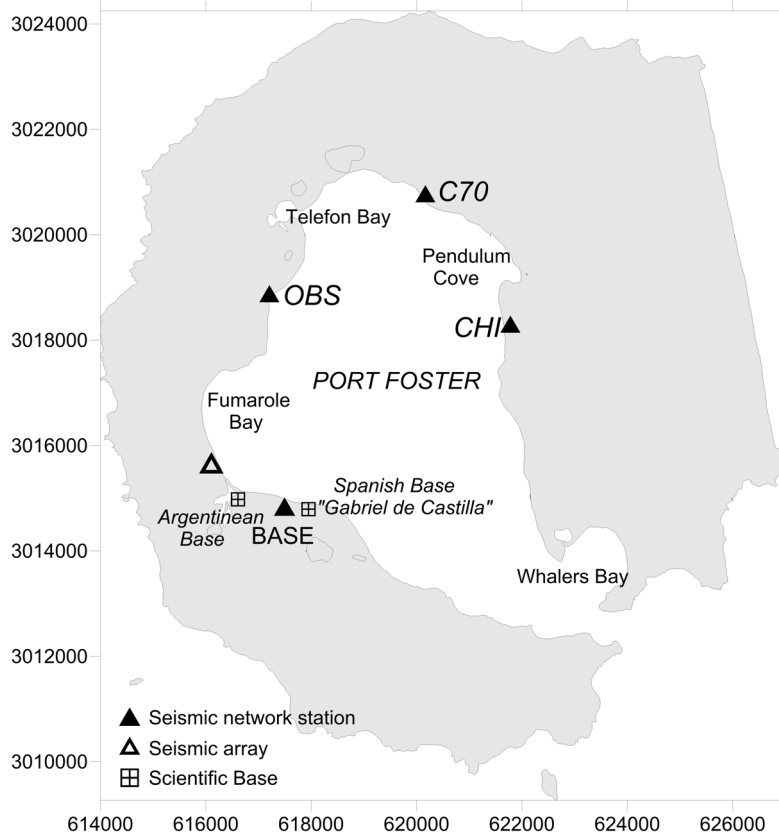
Figure 5. Map of the seismic stations and array used since 2008.

Figure 6. View of Port Foster with photos of the network and array stations.

Figure 7. Left: installation of a three-component Mark Products L4C seismometer; right: installation of a three-component Lennartz 3D/5s seismometer.
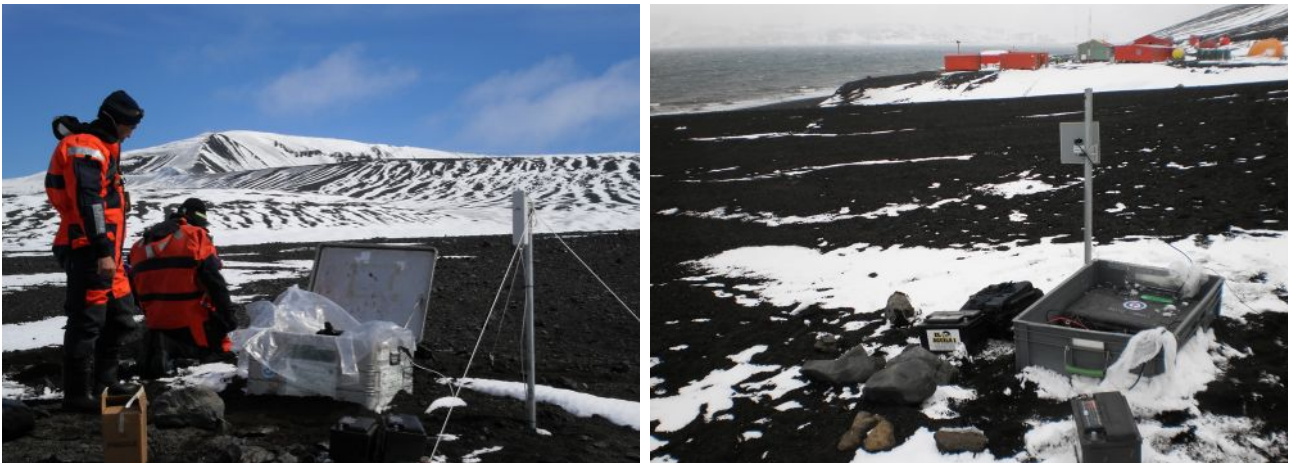

Figure 8. View of the seismic network stations located at Obsidianas Beach (left) and at the Gabriel de Castilla Base (right) during the 2010-2011 survey.

data, and generates summary plots of seismic activity. Moreover, it provides information about the current state of the stations. The 12 data channels received from the 4 stations are stored in miniSEED format. Data are displayed in real time, allowing a rapid and efficient seismo-volcanic surveillance.

4.2. Seismic arrays

Seismic arrays are important tools for volcano monitoring. They allow estimating the dominant apparent slowness vector of the seismic wavefield. We have used seismic arrays since 1994 (Figure 9) to investigate the propagation characteristics and estimate source parameters of LP events, volcanic tremors, and low-magnitude VT earthquakes. The hardware has changed from 8-channel, 16-bit systems (1994-2004) to 12-channel, 24-bit systems (2004-present). Initially, the arrays were not operated as part of the surveillance network, because data recording was local and processing was not optimized. Moreover, they have relatively large power needs (about 26 W) and therefore their maintenance

was a heavy task. Since the International Polar Year, we have put more effort to incorporate the seismic arrays into the monitoring network. Three points had to be improved: (1) make data readily available at the Spanish Base, ideally in real time; (2) reduce power consumption; (3) provide real-time estimates of the apparent slowness vectors in different frequency bands.

The first objective was addressed by connecting the 12-channel data acquisition system to the wireless network using a WiFi antenna. We have developed two prototypes of seismic array. One uses a netbook computer running SeisLog to manage data acquisition and wireless connection. Data are both recorded locally and sent in real time to the Base computer. The system is optimized to reduce power consumption to about 15 W. The second prototype is a simplified version of the original design, lacking the PC and the recording software. Data are transmitted directly from the acquisition module. There is no local recording; therefore data are lost when the wireless connection fails. On the other hand, a great advantage is the low

Figure 9. Left: installation of the array data acquisition system in the Fumarole Bay area during the 2010-2011 survey; right: reference stake indicating the position of one of the seismometers of the 12-channel seismic array deployed in the Fumarole Bay during the 2009-2010 survey.

power consumption (~6 W). Both prototypes of seismic array have been tested in the field during the 2010-2011 and 2011-2012 surveys. After these test, we concluded that the first design with local recording was preferable, despite the larger power required, because it minimizes sporadic data losses.

Since the array includes a three-component station, since the 2011-2012 survey we use it as a fifth recording site of the surveillance network.

4.3. Data analysis

With the current network configuration, three-component data streams are transmitted continuously from the stations to the Base, where they are stored and organized in a database using SEISAN. The array data are available in real time. As mentioned above, the main challenge for the seismologists working at Deception Island is to analyze data as close to real-time as possible. Moreover, we are interested in finding out: (1) the num-
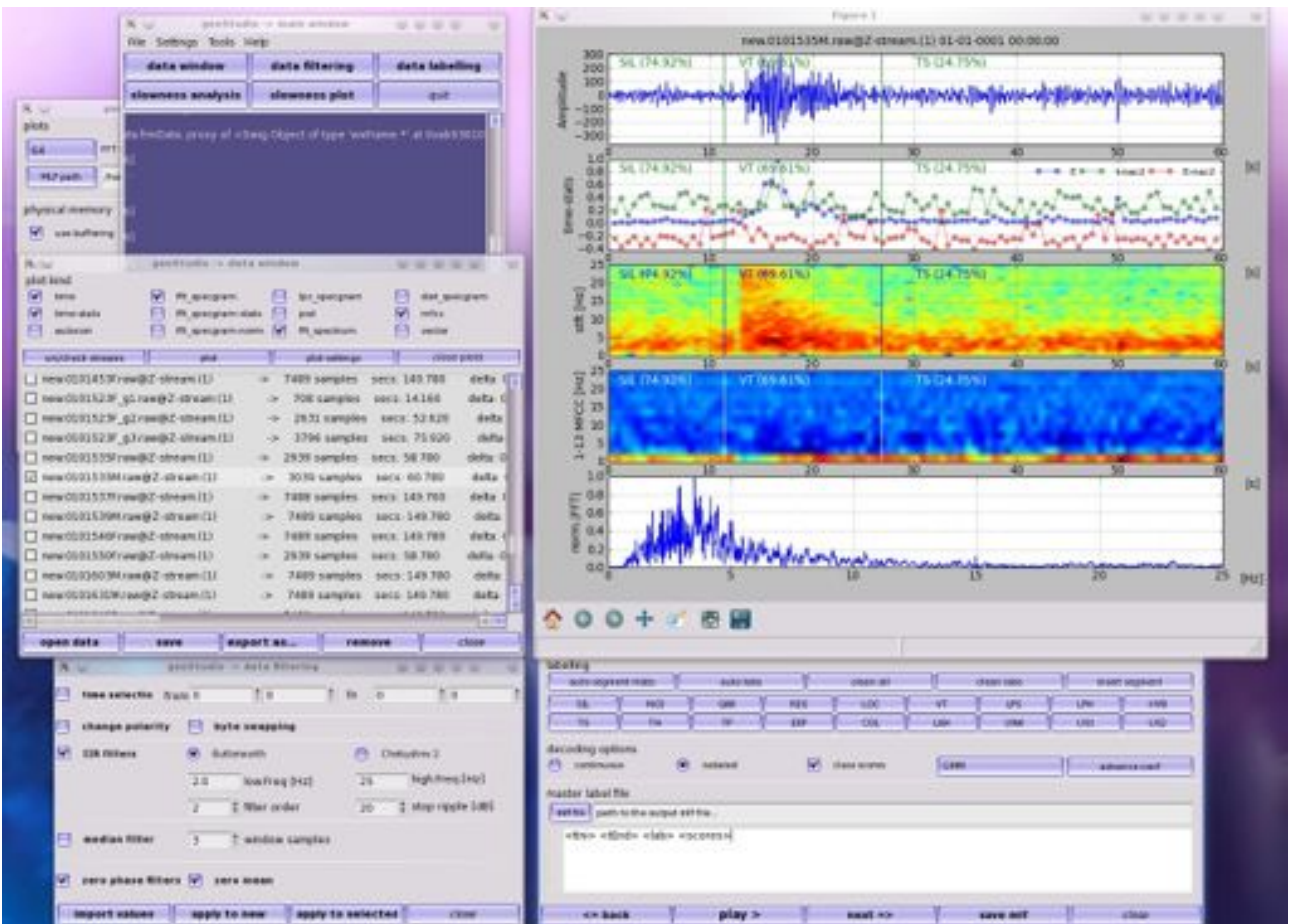

Figure 10. Screenshot of the software for the automatic signal recognition running under the GeoStudio package.

ber and temporal distribution of events; (2) the characteristics of the waveforms (amplitude, duration, envelope, phase arrivals, etc.) and their spectral content; (3) the origin of earthquakes, to distinguish between volcanic and tectonic events; (4) the type of event (VT, LP, hybrid); (5) the frequency content, intensity and duration of volcanic tremor; (6) the source parameters (size, origin time and hypocentral location).

In order to reduce the time required for the analysis of the data, we have developed a software tool, named GeoStudio, which automatically performs some of the above mentioned operations. It has been written in Python/C by G. Cortés, J. Almendros, J.M. Ibáñez and J. Orozco-Rojas at the IAG-UGR. It is a multiplatform software package that runs on any computer with Python interpreter and libraries. It has been tested on several GNU/Linux distributions and Windows releases (XP, Vista, and 7). The package has a modular design that allows the incorporation of new routines developed for different tasks. GeoStudio is able to read and display multichannel data in standard seismic formats (SEISAN, SAC, miniSEED, GSE2) and other formats (RAW, WAV, ASCII, TXT, Q, HTK). It allows for a basic signal processing including byte-swapping, polarity conversions, filtering, offset correction, spectral analysis (spectrum, cepstrum and spectrogram), and has a powerful graphical interface for 1D and 2D plotting.

In the context of volcano surveillance, the most important capabilities recently added to GeoStudio are: (1) an automated recognition tool to detect, identify and classify seismo-volcanic signals; (2) a routine to estimate in near real-time the apparent slowness vectors of the wavefield recorded by a seismic array.

Automatic recognition of seismo-volcanic signals is very useful in early warning systems. Early knowledge of the evolution of the precursory seismic activity can help predicting volcanic eruptions [Chouet 1996]. Since 2002, the IAG-UGR and the Departamento de Teoría de la Señal, Telemática y Comunicaciones of the University of Granada, Spain (TSTC-UGR) are working together to develop a real-time, unsupervised recognition system for volcano monitoring. Most of this work was carried out with data collected at Deception Island volcano since 1994 [Benítez et al. 2007] and data from other volcanoes [Benítez et al. 2009, Cortés et al. 2009a,b].

The event detection and classification tool is based on Hidden Markov Models (HMM) and Gaussian Mixture Models (GMM). These models are applied to real-time data through an unsupervised procedure (summarized in Figure 10) that detects and classifies
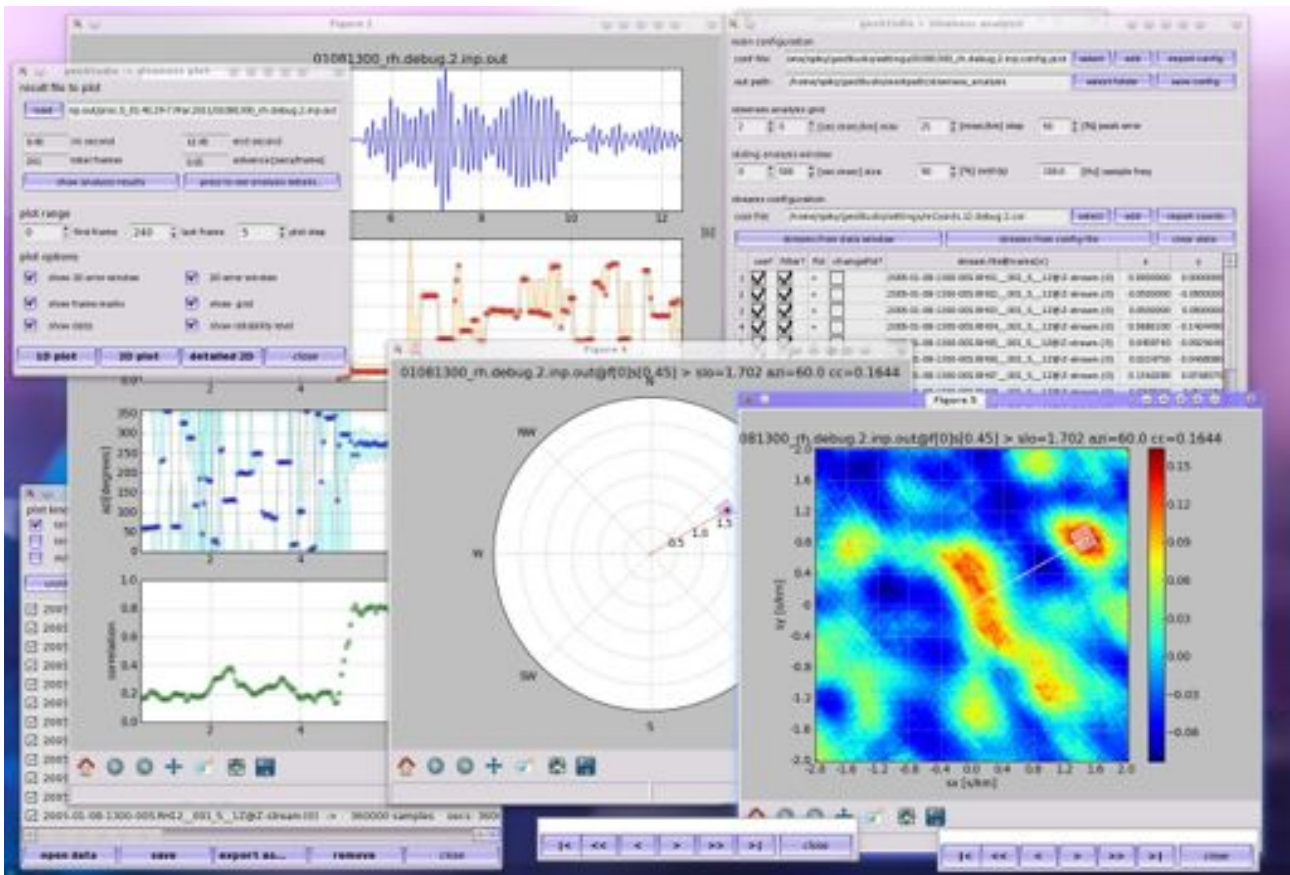

Figure 11. Screenshot of the software for the automatic estimate of the apparent slowness vector used for seismic array data running under the GeoStudio package.

Figure 12. Seismometer (left) and data acquisition system (right) of the permanent station DCP, installed in February 2008 at Deception Island.

events into pre-defined groups (regional earthquakes, VT earthquakes, LP events, hybrids, and volcanic tremor). The current recognition system was successfully tested with the Deception Island seismic database [Benítez et al. 2007, 2009, Cortés et al. 2014]. For example, Benítez et al. [2007] used the 1994-1995, 1995-1996 and 2001-2002 data. They achieved a recognition rate of more than 95% in an unsupervised classification of LP events, and about 90% in real-time applications. The system accuracy scores can be further improved with a parallel-architecture implementation of GMM [Cortés et al. 2014].

GeoStudio also performs automatically the estimate of apparent slowness vectors from array data. The routine is based on the zero-lag cross-correlation (ZLCC) method [Del Pezzo et al. 1997, Almendros et al. 1999]. Calculations are repeated on a moving window whose length depends on the dominant frequency of the signal. Depending on the selected parameters, the analysis could take longer than the streaming of data, which implies that results would be available in near real-time. The result is a time series of the apparent slowness and propagation azimuth (together with error estimates) of the wavefield contained in each window. This information is crucial for the analysis of LP events, volcanic tremor, and low-magnitude VT earthquakes.

GeoStudio provides an intuitive graphical interface that simplifies the selection of parameters for the apparent slowness vector analysis. It is able to produce different types of plots (temporal plots, slowness maps, spatial representation of slowness vectors, etc.) to visualize the results from different points of view (Figure 11). We have also made an effort to optimize the speed of the analysis. For example, the original ZLCC algorithm has been modified to speed up the calculations in case of largely overlapping windows. Moreover, the modular design allows us to implement other algorithms such as MUSIC [Schmidt 1986, Goldstein and Archuleta 1987], a fast frequency-domain method of wavefield decomposition.

The GeoStudio software is continuously developing with new tools and algorithms to improve our ability to analyze the seismo-volcanic data in a fast and effective way.

4.4. Permanent station

Our work at Deception Island volcano until 2007 consisted of periodic temporary surveys carried out during the austral summer. Obviously, this implies that the island was lacking of instrumental coverage for about 75% of the time. Thus we built up a small network of three broadband permanent stations in the south Shetlands - Antarctic Peninsula area in order to extend the temporal coverage of seismic recording. Selected sites were the Spanish Antarctic Bases "Juan Carlos I" and "Gabriel de Castilla", located at Livingston and Deception Islands, respectively, and the Argentinean Base "Primavera", located at Cierva Cove, in the Antarctic Peninsula. Stations are located along an N-S profile about 250 km long, in different geodynamic units. This project had both scientific and technical challenges. Scientific objectives are: (1) to evaluate the level of microseismicity in these areas, both of tectonic and volcanic origin; (2) to provide additional coverage for earthquakes location and other studies coordinated with different seismic networks; (3) to study the seismic characteristics of the selected sites (site effects, attenuation and anisotropy); (4) to calculate receiver functions in order to infer the local crustal structure. Technical challenges are related to the extreme weather conditions and the efficient use of renewable energy sources.

The three stations were deployed in February 2008 and have been working continuously since then with annual maintenances. They are composed of a 16-s electrolytic seismometer Eentec SP400 and a 24-bit datalogger Eentec DR4000 (Figure 12) sampling at 100 sps. Data are stored locally on a 40 Gb hard disk. The main advantage of this station is the extremely low power con-
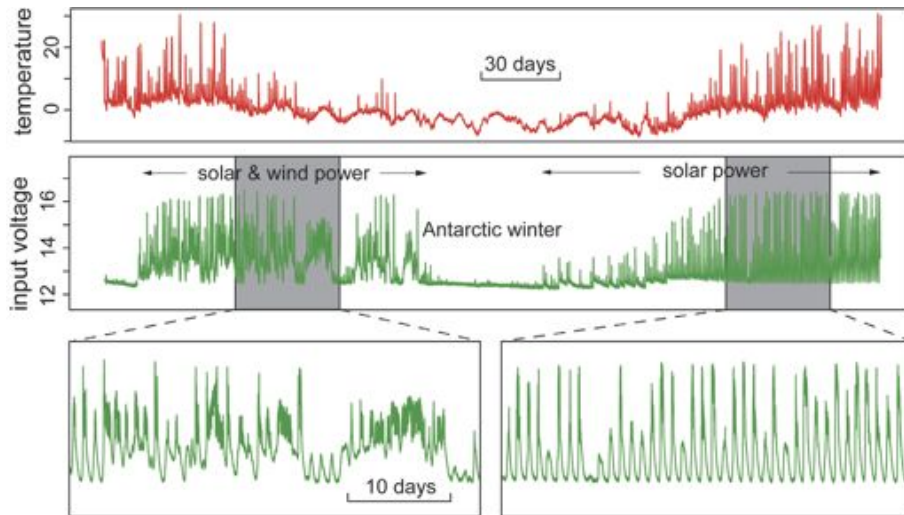
Figure 13. Evolution of system temperature (top, in red) and voltage (middle and bottom, in green) at the seismic station DCP during the year 2008. Zoomed windows (bottom) show the energy supply during periods with inputs from the solar panel and wind generators (bottom left) and from the solar panel only, after the wind generators were smashed during the Antarctic winter (bottom right).

sumption (about 1 W). The electrolytic seismometer offers further advantages: it needs little maintenance (e.g. no need to centre the mass) and is less sensitive to levelling errors than conventional broadband seismometers.

The most important problem that we could foresee was the possibility of fluid freezing in the Antarctic environment. To face this problem, we developed an electronic device that monitors the internal temperature, as well as the battery level and power supply. Basically, the circuit is composed by a real-time clock, two current sensors, a temperature sensor, an ATMEGA64 microcontroller, and a 1 Gb MMC memory. Figure 13 shows an example of the temperature recorded during 2008. Although external temperatures were often well below –20°C, the internal temperature never dropped below –7°C.

At the permanent stations, power is supplied by vertical-axis wind generators and high-efficiency solar panels (Figure 14). We also use a large battery bank (up to 10 batteries of 70 Ah) to confront relatively long periods without energy supply (i.e. without wind or light). However, wind generators at the Deception Island station (named DCP) proved not to be particularly useful. Strong winds, ice, snow, freezing cycles, and the presence of fine pyroclasts contributed to the rapid degradation of the generator gears and blades. Although we replaced the wind generators, they failed again, and since 2009 DCP works only with solar energy. Figure 13 shows the joint contribution of wind generators and solar panel during the first months of 2008, while after the Antarctic winter, only the solar power, clearly recognized by the daily periodic oscillations, contributed to power supply.

In the particular case of Deception Island, the deployment of the permanent station was a great advance in seismic monitoring. Instead of seasonal patches of data, we have collected four years of continuous seismic record. However, a single station has limited applications, for example it cannot be used to estimate source locations. But still, these data have revealed new, interesting features of the seismo-volcanic activity of Deception Island, such as the absence of direct relationship between long-period seismicity and recharge processes in the hydrothermal system, the occurrence of long-lasting volcanic tremor episodes, and the interaction between oceanic microtremors and volcanic earthquakes [Stich et al. 2011, Jiménez 2012].

5. Summary and future challenges

Deception Island is one of the most active volcanoes of the Antarctic region, and among the Antarctic sites that are most visited by tourists. Moreover, two scientific bases operate during the austral summer. For these reasons an efficient monitoring system is needed, and volcano seismology is one of the most useful tools for volcanic surveillance. Our research group from IAG-UGR is accomplishing this task at Deception Island since 1994 using different types of instruments. On the occasion of the International Polar Year, we have been able to improve and update the seismic monitoring system. The most important advances were related to: (1) upgrade the seismic network to efficiently transmit real-time data via WiFi; (2) include the seismic array into the surveillance network; (3) simplify and automate the basic signal processing, including the identification and classification of seismo-volcanic events and the apparent slowness estimates; and (4) extend the temporal coverage of the recording through the installation of a low-power permanent station. However, more issues need to be addressed in the near future, such as the optimization of
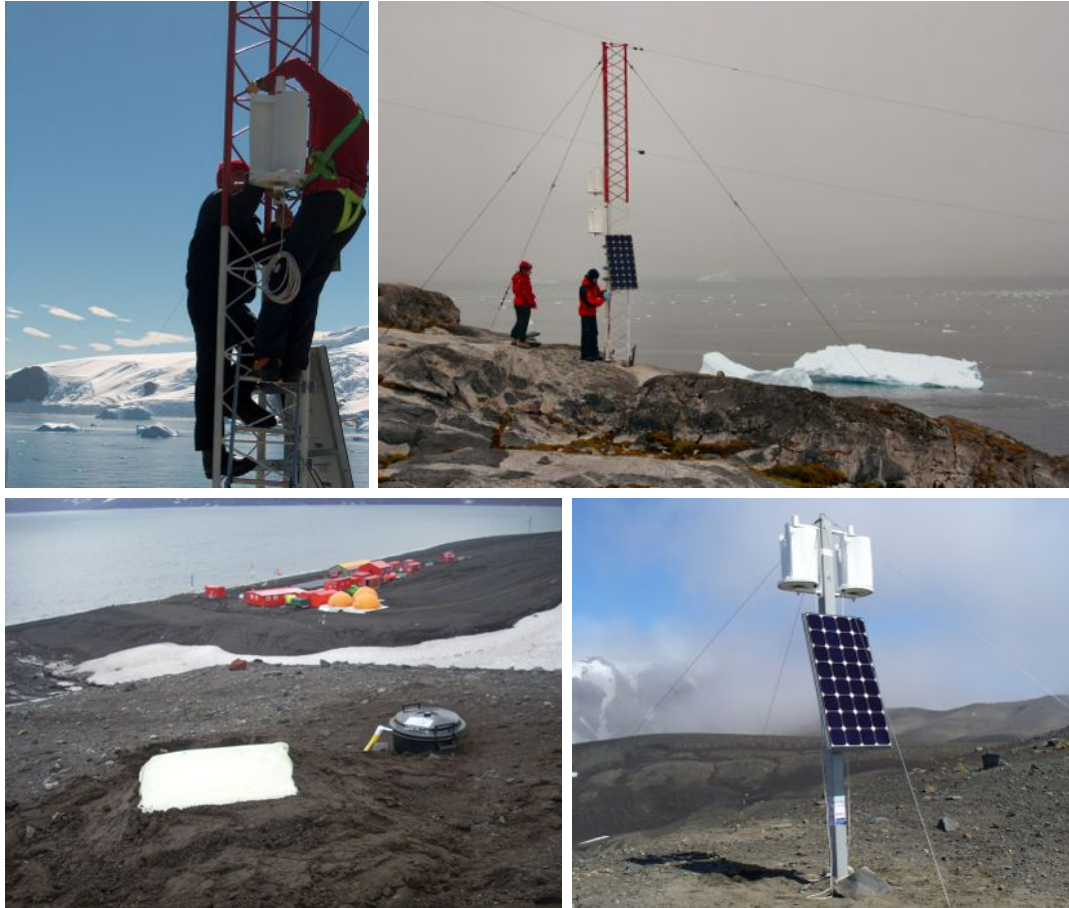
Figure 14. View of the solar panel and wind generators installed at the permanent seismic stations at Cierva Cove (top) and Deception Island (bottom) in February 2008.

the temporary network and seismic array in terms of power efficiency and spatial coverage, the implementation of tools for real-time processing, and the installation of new permanent stations with real-time data trans-

mission. The temporary network and the seismic array require periodic maintenance and battery replacement. A higher power efficiency combined with the use of solar panels would stretch remarkably the autonomy of
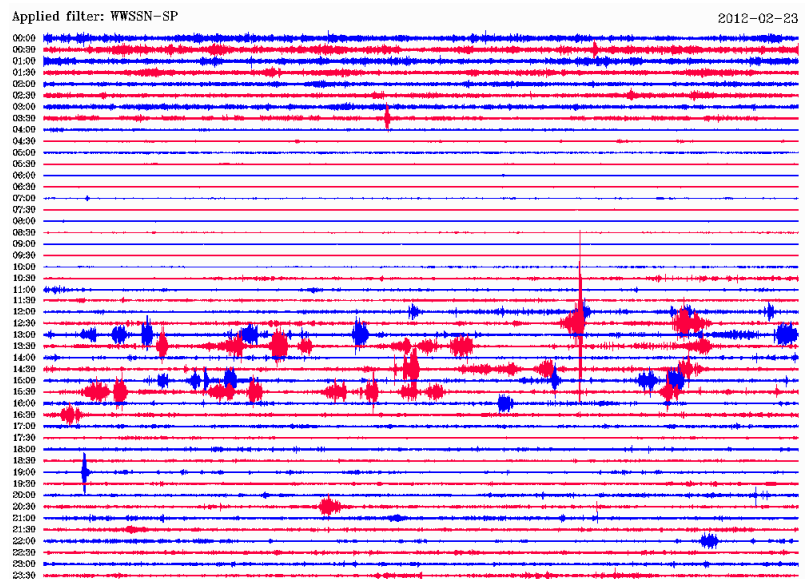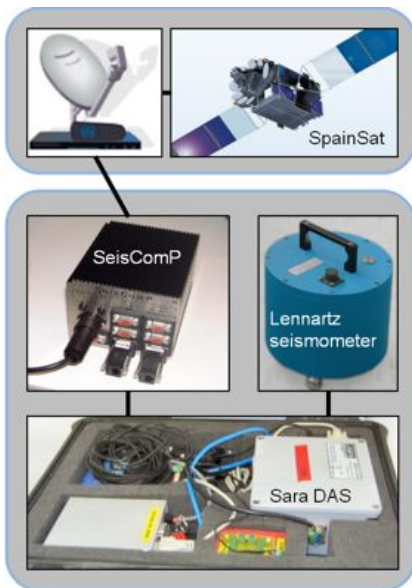

Figure 15. Left: elements of the system designed for satellite transmission of seismic data during the austral winter; right: example of a 24-hour record image generated by SeisComP and transmitted successfully from Deception Island to the IAG-UGR in Spain during a test of the system on February 23, 2012.

the stations. On the other hand, the spatial coverage of the network, now limited to the northern half of Port Foster, will be hopefully extended to the southern part of the island. In the last 4 years, the permanent station DCP has provided interesting data from March to November, when the Spanish Base is closed, showing that seismic activity has been very intense in certain periods. However, we cannot determine hypocentral locations unless we install other permanent stations. As for the possibility of transmitting data during the winter, we have developed a prototype seismic station in collaboration with the Spanish Army operating at the Gabriel de Castilla Base (Figure 15). This station, linked to a router using the software SeisComP, is able to send data through the Spanish government satellite SpainSat. However, the huge amount of raw seismic data leads us to a more realistic alternative: SeisComP produces a 24-hour record image that can be downloaded and sent to IAG-UGR. The system capabilities were tested in February 2012, during the 2011-2012 survey. In this test, images of the daily seismic activity were successfully produced and transmitted from Deception Island to the IAG-UGR in Spain. This procedure allows us to check the level of seismic activity at the Deception Island volcano on a daily basis, even during winter, when the Base is closed. This information is also useful for assessing the level of volcanic activity at the beginning of the periodic summer surveys, when scientific/technical staff is on the way to the Gabriel de Castilla Base.

References

Abril, M. (2007). Evolución, diseño y desarrollo de antenas sísmicas. Las antenas del Gran Sasso, del Vesubio y las nuevas antenas sísmicas portátiles del Instituto Andaluz de Geofísica. Aplicación a zonas tectónicas y volcánicas, PhD Thesis, University of Granada, Spain.

Alguacil, G., J. Almendros, E. Del Pezzo, A. García, J.M. Ibáñez, M. La Rocca, J. Morales and R. Ortiz (1999). Observations of volcanic earthquakes and tremor at Deception Island, Antarctica, Annali di Geofisica, 3, 417-436.

Almendros, J., J.M. Ibáñez, G. Alguacil, E. Del Pezzo and R. Ortiz (1997). Array tracking of the volcanic tremor source at Deception Island, Antarctica, Geo-phys. Res. Lett., 24, 3069-3072.

Almendros, J., J.M. Ibáñez, G. Alguacil and E. Del Pezzo (1999). Array analysis using circular wavefront geometry: An application to locate the nearby seismo-volcanic source, Geophys. J. Int., 136, 159-170.

Almendros, J., E. Carmona and J.M. Ibáñez (2004). Precise determination of the relative wave propagation parameters of similar events using a small aperture seismic array, J. Geophys. Res., 109, B11308; doi:10.1029/2003JB002930.

Baker, P.E., I. McReath, M.R. Harvey, M.J. Roobol and T.G. Davis (1975). The Geology of the South Shetland Islands: V. Volcanic evolution of Deception Island, British Antarctic Survey Scientific Reports, 78, 81.

Baraldo, A., and C.A. Rinaldi (2000). Stratigraphy and structure of Deception Island, south Shetland Island, Antarctica, J. South Am. Earth Sci., 13, 785-796.

Benítez, M.C., J. Ramírez, J.C. Segura, J.M. Ibáñez, J. Almendros, A. García-Yeguas and G. Cortés (2007). Continuous HMM-based seismic event classification at Deception Island, Antarctica, IEEE Trans. Geosci. Rem. Sens., 45, 138-147.

Benítez, M.C., J.M. Ibáñez, L. García, G. Cortés and I. Álvarez (2009). Analysis of volcanic seismicity at Deception Island, Stromboli volcano and Mt. Etna using an automatic CHMM-based recognition method, In: C.J. Bean, A.K. Braiden, I. Lokmer, F. Martini and G.S. O'Brien (eds.), The VOLUME project - Volcanoes: Understanding subsurface mass Movement, 140-149; ISBN:978-1-905254-39-2.

Berrocoso, M., A. Fernández-Ros, M.A. Ramírez, J.M. Salamanca, C. Torrecillas, A. Pérez-Peña, R. Páez, A. García-García, Y. Jiménez-Teja, F. García-García, R. Soto, J. Gárate, J. Martín-Dávila, A. Sánchez-Arzola, A. de Gil, J.A. Fernández-Prada and B. Jigena (2008). Geodetic research on Deception Island and its environment (South Shetland Islands, Bransfield Sea and Antarctic Peninsula) during Spanish Antarctic campaigns (1987-2007), In: A. Capra and R. Dietrich (eds.), Geodetic and Geophysical Observations in Antarctica, 97-123.

Carmona, E., J. Almendros, J.A. Peña and J.M. Ibáñez (2010). Characterization of fracture systems using precise array locations of earthquake multiplets: An example at Deception Island volcano, Antarctica, J. Geophys. Res., 115, B06309; doi:10.1029/2009JB006865.

Carmona, E., J. Almendros, I. Serrano, D. Stich and J.M. Ibáñez (2012). Results of seismic monitoring surveys at Deception Island Volcano (Antarctica), from 1999-2011, Antarctic Science, 24; doi:10.1017/S0954102012000314.

Caselli, A.T., M. Santos-Afonso and M.R. Agusto (2004).

Gases fumarólicos de la isla Decepción (Shetlands del Sur, Antártida): variaciones químicas y depósitos vinculados a la crisis sísmica de 1999, Rev. Asoc. Geol. Arg., 59, 291-302.

Caselli, A.T., G. Badi, A.L. Bonatto, C.L. Bengoa, M.R. Agusto, A. Bidone and J.M. Ibáñez (2007). Actividad sísmica y composición química fumarólica anómala debido a posible efecto sello en el sistema volcánico, Isla Decepción (Antártida), Rev. Asoc. Geol. Arg., 62, 545-552.

Chouet, B. (1992). A seismic model for the source of long-period events and harmonic tremor, In: K. Aki, P. Gasparini and R. Scarpa (eds.), Volcanic Seismology, IAVCEI Proceedings in Volcanology 3, Springer, 133-156.

Chouet, B. (1996). Long-period volcano seismicity: its source and use in eruption forecasting, Nature, 380, 309-316.

Correig, A.M., M. Urquizu, J. Vila and J. Martí (1997). Analysis of the temporal occurrence of seismicity at Deception Island (Antarctica). A nonlinear approach, Pure Appl. Geophys., 149, 553-574.

Cortés, G., R. Arámbula, L.A. Gutiérrez, C. Benítez, J.M. Ibáñez and P. Lesage (2009a). Evaluating robustness of an HMM-based classification system of volcano-seismic events at Colima and Popocatépetl volcanoes, IEEE International Geoscience and Remote Sensing Symposium.

Cortés, G., R. Arámbula, I. Álvarez, M.C. Benítez, J.M. Ibáñez, P. Lesage, M. González Amezcua and G. Reyes Dávila (2009b). Analysis of Colima, Popocatépetl and Arenal volcanic seismicity using an automatic CHMM-based recognition, In: C.J. Bean, A.K. Braiden, I. Lokmer, F. Martini and G.S. O'Brien (eds.), The VOLUME project - Volcanoes: Understanding subsurface mass Movement, 150-160; ISBN:978-1-905254-39-2.

Cortés, G., L. García, I. Álvarez, C. Benítez, A. de la Torre and J. Ibáñez (2014). Parallel System Architecture (PSA): An efficient approach for automatic recognition of volcano-seismic events, J. Volcanol. Geoth. Res., 271, 1-10; doi:10.1016/j.jvolgeores.2013.07.004.

Del Pezzo, E., M. La Rocca and J.M. Ibáñez (1997). Observations of high-frequency scattered waves using dense arrays at Teide volcano, B. Seismol. Soc. Am., 87, 1637-1647.

Fernández-Ibáñez, F., R. Pérez-López, J.J. Martínez-Díaz, C. Paredes, J.L. Giner-Robles, A. Caselli and J.M. Ibáñez (2005). Costa Recta Beach, Deception Island, West Antartica: a retreated scarp of a submarine fault?, Antarctic Science, 17, 418-426.

García, A., I. Blanco, J.M. Torta, M. Astiz, J.M. Ibáñez and R. Ortiz (1997). A search for the volcanomagnetic signal at Deception volcano (South Shetland Islands, Antarctica), Annali di Geofisica, 40, 319-327.

García-Yeguas, A., J. Almendros, R. Abella and J.M. Ibáñez (2011). Quantitative analysis of seismic wave propagation anomalies in azimuth and apparent slowness at Deception Island volcano (Antarctica) using seismic arrays, Geophys. J. Int., 184, 801-815.

Goldstein, P., and R.J. Archuleta (1987). Array analysis of seismic signals, Geophys. Res. Lett., 14, 13-16.

González-Casado, J.M., J. López-Martínez, J. Giner, J.J. Durán and P. Gumiel (1999). Análisis de la microfracturación en la isla Decepción, Antártida occidental, Geogaceta, 26, 27-30.

Guirao, J.M., G. Alguacil, F. Gómez, F. Vidal and F. De Miguel (1990). An automatic process for phase picking, location and magnitude estimation of local events, Cahiers du Centre Européen de Géodynamique et de Séismologie, 1, 55-64.

Havskov, J., and L. Ottemöller (1999). SEISAN, Earthquake Analysis Software for Windows, Sun and Linux: Manual and software, Institute of Solid Earth Physics, University of Bergen.

Havskov, J., J.A. Peña, J.M. Ibáñez, L. Ottemöller and C. Martínez-Arévalo (2003). Magnitude scales for very local earthquakes. Application for Deception Island volcano (Antarctica), J. Volcanol. Geoth. Res., 128, 115-133.

Havskov, J., and G. Alguacil (2004). Instumentation in Earthquake Seismology, In: Modern approaches in Geophysics, 22, Springer.

Ibáñez, J.M., J. Morales, G. Alguacil, J. Almendros, R. Ortiz and E. Del Pezzo (1997). Intermediate focus earthquakes under South Shetland Islands, Antarctica, Geophys. Res. Lett., 24, 531-534.

Ibáñez, J.M., E. Del Pezzo, J. Almendros, M. La Rocca, G. Alguacil, R. Ortiz and A. García (2000). Seismovolcanic signals at Deception Island volcano, Antarctica: wavefield analysis and source modelling, J. Geophys. Res., 105, 13905-13931.

Ibáñez, J.M., J. Almendros, E. Carmona, C. Martínez-Arévalo and M. Abril (2003a). The recent seismo-volcanic activity at Deception Island volcano, Deep-Sea Res. II, 50, 1611-1629.

Ibáñez, J.M., E. Carmona, J. Almendros, G. Saccorotti, E. Del Pezzo, M. Abril and R. Ortiz (2003b). The 1998-1999 seismic series at Deception Island volcano, Antarctica, J. Volcanol. Geoth. Res., 128, 65-88.

Jiménez, V. (2012). Análisis de datos sísmicos del volcán Isla Decepción, Antártida: Resultados de un sismómetro permanente de banda ancha, M.Sc. Thesis, University of Granada, Spain, 205 pp.

Julian, B.R. (1994). Volcanic tremor: Nonlinear excitation by fluid flow, J. Geophys. Res., 99, 11859-11877.

Konstantinou, K.I., and V. Schlindwein (2002). Nature, wavefield properties and source mechanism of volcanic tremor: a review, J. Volcanol. Geoth. Res., 119, 161-187.

Lahr, J., B. Chouet, C. Stephens, J. Power and R. Page (1994). Earthquake classification, location, and error analysis in a volcanic environment; implications for the magmatic system of the 1989-1990 eruptions at Redoubt Volcano, Alaska, J. Volcanol. Geoth. Res., 62, 137-151.

Luzón, F., J. Almendros and A. García-Jerez (2011). Shallow structure of Deception Island, Antarctica, from correlations of ambient seismic noise on a set of dense seismic arrays, Geophys. J. Int., 185, 737-748.

Martí, J., J. Vila and J. Rey (1996). Deception Island (Bransfield Strait, Antarctica): an example of volcanic caldera developed by extensional tectonics, J. Geol. Soc. London, 110, 253-265.

Martínez-Arévalo, C., F. Bianco, J.M. Ibáñez and E. Del Pezzo (2003). Shallow seismic attenuation and shear-wave splitting in the short period range of Deception island volcano (Antarctica), J. Volcanol. Geoth. Res., 128, 89-113.

Ortiz, R., J. Vila, A. García, J. González-Camacho, J.L. Díez-Gil, A. Aparicio, R. Soto, J.G. Viramonte, C. Risso and I. Petrinovic (1992). Geophysical features of Deception Island, In: Recent Progress in Antarctic Earth Science, Terra Scientific Publishing Company, Tokyo, 143-152.

Ortiz, R., G. Alguacil, E. Del Pezzo and J.C. Olmedillas (1994). Array modular de ocho canales, In: R. Ortiz (ed.), Instrumentación en Volcanología II, Servicio de Publicaciones del Cabildo de Lanzarote, 63-84.

Ortiz, R., A. García, A. Aparicio, I. Blanco, A. Felpeto, R. Del Rey, M.T. Villegas, J.M. Ibáñez, J. Morales, E. Del Pezzo, J.C. Olmedillas, M. Astiz, J. Vila, M. Ramos, J.G. Viramonte, C. Risso and A. Caselli (1997). Monitoring of the volcanic activity of Deception Island, South Shetland Islands, Antarctica (1986-1995), In: The Antarctic Region: Geological Evolution and Processes, 1071-1076.

Pelayo, A.M., and D.A. Wiens (1989). Seismotectonics and relative plate motions in the Scotia Sea region, J. Geophys. Res., 94, 7293-7320.

Rey, J., L. Somoza and J. Martínez-Frías (1995). Tectonic, volcanic, and hydrothermal event sequence on Deception Island (Antarctica), Geo-Marine Letters, 15, 1-8.

Robertson-Maurice, S.D., D.A. Wiens, P.J. Shore, E. Vera and L.M. Dorman (2003). Seismicity and tectonics of the South Shetland Islands and Bransfield Strait from a regional broadband seismograph deployment, J. Geophys. Res., 108; doi:10.029/2003JB002416.

Roobol, M.J. (1973). Historic volcanic activity at Deception Island, British Antarctic Survey Bull., 32, 23-30.

Saccorotti, G., J. Almendros, E. Carmona, J.M. Ibáñez and E. Del Pezzo (2001). Slowness anomalies from two dense seismic arrays at Deception Island volcano, Antarctica, B. Seismol. Soc. Am., 91, 561-571.

Schmidt, R.O. (1986). Multiple emitter location and signal parameter estimation, IEEE Trans. Ant. Prop., 34, 276-280.

Smellie, J.L. (1988). Recent observations on the volcanic history of Deception Island, South Shetland Islands, British Antarctic Survey Bull., 81, 83-85.

Smellie, J.L., and J. López-Martínez (2002). Geological and geomorphologycal evolution: summary, In: J. López-Martínez, J.L. Smellie, J.W. Thomson and M.R.A. Thomson (eds.), Geology and Geomorphology of Deception Island, BAS GEOMAPS Series, Cambridge.

Stich, D., J. Almendros, V. Jiménez, F. Mancilla and E. Carmona (2011). Ocean noise triggering of rhythmic long-period events at Deception Island volcano, Geophys. Res. Lett., 38, L22307; doi:10.1029/2011GL049671.

Utheim, T., and J. Havskov (1999). The SeisLog Data Acquisition System, Version 8.1, manual, Institute of Solid Earth Physics, University of Bergen, Norway, 105 pp.

Vila, J., J. Martí, R. Ortiz, A. García and A.M. Correig (1992). Volcanic tremors at Deception Island (South Shetland Islands, Antarctica), J. Volcanol. Geoth. Res., 53, 89-102.

Vila, J., A.M. Correig and J. Martí (1995). Attenuation and source parameters at Deception Island (South Shetland Islands, Antarctica), Pure Appl. Geophys., 144, 229-250.

Walker, G.P.L. (1984). Downsag calderas, ring faults, caldera sizes, and incremental caldera growth, J. Geophys. Res., 89, 8407-8416.

Zandomeneghi, D., A. Barclay, J. Almendros, J.M. Ibáñez, W.S.D. Wilcock and T. Ben-Zvi (2009). The crustal structure of Deception Island Volcano from P-wave seismic tomography: tectonic and volcanic implications, J. Geophys. Res., 114, B06310; doi:10.1029/2008JB006119.

*Corresponding author: Javier Almendros,
Instituto Andaluz de Geofísica, Universidad de Granada,
Granada, Spain; email: alm@iag.ugr.es.